Allosteric non-competitive small molecule selective inhibitors of CD45 tyrosine phosphatase suppress T-cell receptor signals and inflammation in vivo

Michael Perron, Shafinaz Chowdhury, Isabelle Aubry, Enrico Purisima, Michel L. Tremblay, H. Uri Saragovi

Lady Davis Institute-Jewish General Hospital; McGill University; Montreal, Quebec, H3T 1E2; Canada. (MP, SC, HUS)

Department of Pharmacology & Therapeutics; McGill University; Montreal, Quebec, H3G 1Y6; Canada. (MP, HUS)

Department of Biochemistry; McGill University; Montreal, Quebec, H3G 1Y6; Canada. (IA, EP, MLT)

Department of Oncology; McGill University; Montreal, Quebec, H3G 1Y6; Canada. (HUS)

Goodman Cancer Research Center; McGill University; Montreal, Quebec, H3G 1Y6; Canada. (MLT)

Segal Cancer Center; McGill University; Montreal, Quebec, H3T 1E2; Canada. (HUS)

Biotechnology Research Institute, National Research Council Canada; Montreal, QC H4P 2R2 (EP)

1

Runnning title

Selective inhibitors of CD45 PTPase

Corresponding Author Contact

Dr. H. Uri Saragovi

Professor, McGill University

Lady Davis Institute-Jewish General Hospital

3755 Cote St. Catherine. E-535

Montreal, Quebec - CANADA   H3T 1E2

(514) 340-8222   x 5055 (office)

 (514) 340-8717 (FAX)

email: Uri.Saragovi@mcgill.ca

Statistics:

37 pages

1 table

6 figures

Number of words in Abstract: 147

Number of words in Introduction: 622

Number of words in Discussion: 1,151

Number of References: 41

6 supplemental figures + 2 supplemental tables

Non-standard abbreviations

1,2-napthoquinone : 1,2-NQ

circular dichroism : CD

delayed type hypersensitivity : DTH

Generalised Amber Force Field : GAFF

ovalbumin : OVA

phosphotyrosine : pY

protein tyrosine phosphatase : PTP

solvated interaction energy : SIE

T Cell Receptor : TCR

ABSTRACT

CD45 is a receptor-like member of the protein tyrosine phosphatase (PTP) family. We screened *in silico* for small molecules binding at a predicted allosteric pocket unique to the CD45 intracellular domain, and validated inhibitors by *in vitro* phosphatase assays. One compound **211** exhibited CD45 IC_{50} 200 nM and had >100-fold selectivity over six related PTPs. The relevance of the allosteric pocket was verified through site directed mutagenesis. Compound **211** has a non-competitive mechanism of action, and it is extremely effective at preventing dephosphorylation of substrate Lck pY-505 versus preventing dephosphorylation of Lck pY-393. In cultured primary T cells, **211** prevents T-cell receptor-mediated activation of Lck, Zap-70 and MAPK, and IL-2 production. In a delayed-type hypersensitivity reaction *in vivo*, compound **211** abolished inflammation. This work demonstrates a novel approach to develop effective allosteric inhibitors that can be expanded to target the corresponding allosteric domains of other receptor PTPs.

4

Introduction

CD45 is a transmembrane receptor-like protein tyrosine phosphatase (PTP), expressed on cells of hematopoietic origin. The function of CD45 is to regulate signal transduction and T cell activation in response to antigen stimulation at the T Cell Receptor (TCR) (Justement, 1997). CD45 exists as a variably glycosylated extracellular domain with no known physiological ligand (Streuli et al., 1987), and a cytoplasmic portion with tandem D1 and D2 domains (Glover and Tracey, 2000). D1 is the catalytically active domain, as it harbors the cysteine residue involved in the enzymatic reaction that hydrolyzes phosphate from tyrosine residues. D2 is catalytically inactive (Streuli et al., 1990).

CD45 regulates the phosphorylation of the Src-family kinases such as Lck and Fyn, as well as ζ-ITAM of the CD3 component of the TCR. In T cells, proper activation of Lck causes rapid Ca^{++} fluxes and the phosphorylation of Zap-70 and Erk; which then stimulate the production of IL-2. These are standard readouts for T-cell activation and CD45 activity (Alexander, 2000; Thomas and Brown, 1999). CD45-deficient T cells have diminished proliferation and cytokine production in response to TCR stimulation (Pingel and Thomas, 1989). Furthermore, mutations in the human CD45 gene have been associated with autoimmune diseases such as SCID and multiple sclerosis (Jacobsen et al., 2000; Kung et al., 2000). All these events implicate CD45 as playing a key role in lymphocyte development and activation (Trowbridge and Thomas, 1994).

Full activation of Lck requires the dephosphorylation of an inhibitory tyrosine 505 (pY-505). Dephosphorylation of Lck pY-505 by CD45 facilitates Lck autophosphorylation at an activating tyrosine Lck pY-393. The activating Lck pY-393 is

5

also under CD45 regulation. Thus, CD45 essentially functions as a rheostat to keep Lck in a 'primed' state, ready for activation (Hermiston et al., 2003) but avoiding sustained hyperactivation (D'Oro et al., 1996).

Drug inhibitors of CD45 would disrupt the rheostat and could cause immunosuppression. Competitive CD45 inhibitors that block substrates from docking (Beers et al., 1997) and substrate analogs that poison the catalytic pocket have been reported (Urbanek et al., 2001), with *in vitro* IC50s ~0.2 µM and activity in anti-proliferative assays. One competitive inhibitor (a benzimidazole derivative) had effects on histamine release from rat peritoneal mast cells (Hamaguchi et al., 2001). Unfortunately, these CD45 inhibitors are not clinically useful. One general problem of competitive inhibitors is their poor selectivity because many phosphatases share substrates and/or the structure of the catalytic pocket (Blaskovich, 2009), and since they usually are charged this prevents efficient entry into cells.

As an alternative, allosteric inhibitors of CD45 could have different mechanisms of action and potentially higher selectivity (Hardy and Wells, 2004), if the allosteric docking site is a structure unique for CD45. We sought to develop selective inhibitors of CD45 that bind to an allosteric intracellular site.

D1 is the catalytically active domain while D2 is catalytically inactive but contributes to the overall secondary structure of intracellular CD45 (Glover and Tracey, 2000; Streuli et al., 1990). The D2 domain regulates the activity of the D1 domain positively and negatively (Felberg and Johnson, 1998), and can impact on the signals downstream of the TCR (Greer et al., 2001; Kashio et al., 1998; Wang et al., 1999). D1 and D2 are connected by a "linker" domain that is unstructured, but which stabilizes a D1-D2

6

interface that forms a network of hydrogen bonds, hydrophobic interactions, and salt bridges (Nam et al., 2005).

We hypothesized that a molecule docking near the linker or D1-D2 interface could act as an allosteric CD45 phosphatase modulator. Here, we report the design, optimization, and characterization of selective allosteric inhibitors of CD45 that are active *in vitro*, *ex vivo* and *in vivo*. We propose that the approach may be expanded to develop inhibitors for other receptor PTPs.

7

Materials & Methods

CD45 Target Structure for Docking Studies

Structure manipulation and visualization were done using SYBYL 7.3 (Tripos, Inc., St. Louis, MO). The crystal structure of domains D1 and D2 of CD45 bound to phosphopeptide qITAM-1 was used (PDB code 1YGR). The bound phosphopeptide was removed and all selenium methionines were replaced by methionine. The crystallographic water molecules and other hetero-atoms were removed from the file. The program Reduce, version 3.1 (Word et al., 1999) was used to add hydrogen atoms to the target atoms and optimize the orientation of the polar hydrogens. Both N- and C- termini of the protein were modeled in the ionized state. All histidine residues were protonated and the catalytic cysteine was modeled as a thiolate.

Database for screening.

The three dimensional structures of NCI (Release 3) compounds were generated by using the CONCORD module of Sybyl. GAFF (Generalised Amber Force Field) atom types and parameters were assigned to the first 120,000 compounds using the antechamber module of AMBER (Case et al., 2005). Partial charges of the compounds were calculated by the AM1-BCC method (Jakalian et al., 2002).

Docking of NCI compounds

The NCI compound library was docked using OMEGA version 2.2 and FRED version 2.0 (OpenEye Scientific Software, Inc.). OMEGA generated multiple low-energy conformers of each compound, which were then docked by FRED into the allosteric cavity present in CD45 phosphatase. Hundred poses for each conformer were kept. These

poses were then re-scored by using the solvated interaction energy (SIE) function (Naim et al., 2007) as shown in Eq. (1):

$$\Delta G_{bind} = \alpha \cdot \left[\; E_C + \Delta G_{bind}^R + E_{vdw} + \gamma \cdot \Delta MSA \; \right] + C \qquad (1)$$

ΔG_{bind}^R is the change in the reaction field energy between the bound and free states, calculated by solving the Poisson equation with the boundary element method program BRI BEM (Purisima, 1998) using a molecular surface generated with a variable-radius solvent probe (Bhat and Purisima, 2006). The ΔMSA term is the change in molecular surface area upon binding. Default values of the parameters were used (Cui et al., 2008). Further docking of the top-scoring poses were done with an in-house docking program WILMA (Naim et al., 2007).

Final selection of compounds for experimental testing were based not only on SIE top scores, but also on visual inspection of the binding mode (shape complementarity between target and ligand, electrostatic interaction and the chemical nature of the compounds.

2-D similarity search

For two of the experimentally validated hits, we carried out a 2-D similarity search of a drug-like subset of the ZINC database (Irwin and Shoichet, 2005) to find molecules that are structurally similar to query compounds. The UNITY program version 7.3.5 (Tripos Inc., St. Louis, Missouri) was used for this search, with Tanimoto coefficients 0.70 and 0.75 for compounds 34932 (**28p**) and 45739 (**37p**), respectively. A total of 34 analogues of 34932 (**28p**) and 36 analogues of 45739 (**37p**) were procured for testing in biological assays.

Compounds

Initial "hit" compounds, including **28p**, **37p** and **57p**, were obtained from the NCI. Compounds **210** and **211** were purchased from Chembridge (San Diego), while **214**, **215** and **216** were purchased from InterBioScreen (Moscow). Stocks of 4 mM were prepared in DMSO, with dilutions made in HBSS. DMSO vehicle control was used in each assay. Competitive CD45 inhibitor RWJ-60475 (Enzo Lifesciences) was a positive control. Quality control and purity of compounds were verified by HPLC and mass spectrometry, and where indicated, also by NMR.

In vitro phosphatase assay

Enzymatic activity of CD45 was assayed using a modified version of the Malachite Green Assay (30), using the CD45 Drug Discovery Kit (Enzo Lifesciences). CD45 phosphatase was pre-incubated with test compounds or controls for 10 minutes in the wells of a 96-well plate before addition of 1 mM phosphorylated substrate, the negative regulatory position of pp60-Src. The reaction proceeded for 20 minutes, before addition of Biomol Green reagent, and spectrophotometric quantification of phosphate content at 620 nm in a Benchmark Plus microplate spectrophotometer (BioRad) with blanks subtracted. For assays with DIFMUP substrate, phosphatase activity was quantified by measuring the fluorescence of its reaction product at 350nm/455nm. The signal to noise ratios were always >5-fold, and the assays were in the linear range.

To determine the mode of CD45 inhibition, we tested various concentrations of inhibitor with three different amounts of peptide substrate. The inhibitor and substrate were added simultaneously, and the reaction was stopped after 20 minutes. A double-reciprocal Lineweaver-Burk plot of $1/V_o$ versus $1/S_o$ revealed the mode of inhibition.

10

To determine the reversibility of CD45 inhibition, absorbance was monitored for 120 minutes, and data collected at various time points were plotted for each peptide substrate with and without the CD45 inhibitor.

Control phosphatases used in counterassays

PTP1B (accession number NM_002827, AA 1-321), SHP-1 (NM_002828, AA 1-354), MKPX (AF165519, full length AA 1-184), LARD1D2 (ENST00000359947, AA 1301-1907), SigmaD1D2 (BC104812, AA 883-1501), PEP (NM_015967, AA 1-323), and PEST (BC051980, AA 1-454) were cloned in pGEX with a GST tag, expressed in DH5α and purified in-house. Control LYP (PTPN22) is the W620 full-length clone, provided by Nunzio Bottini (USC, California), cloned in pGEX 2TK (ENST00000359785, AA 1-807).

Assays to quantify oxidation

CD45 and PTP1B were incubated with either 50 µM **211** or 1,2-naphtoquinone (Sigma), or vehicle at a molar stoichiometry of 50 µM compound per 13 µM enzyme (Iwamoto et al., 2007). After 10 minutes, the reaction was stopped and free thiol content was quantified by addition of 0.2 mM DTNB and 0.75% SDS. After 2 minutes, the concentration of thionitrobenzoic acid, as a measure of thiol content, was determined spectrophotometrically at 412 nm (Riddles et al., 1983).

Cell lines and cell culture

Human leukemia cell lines Jurkat and J45.01 were kindly provided by Dr. Pauline Johnson (University of British Columbia, Vancouver, Canada). J45.01 is a CD45-negative variant of Jurkat cells, and exhibits impaired TCR signalling (Koretzky et al.,

1991). The KB line is a human nasopharyngeal cell. EL4 cells are a mouse thymoma. HEK293 are human kidney cells.

Cellular activation, treatment, lysis, and immunoblotting

Splenocytes prepared from young adult female C57/BL6 mice were semi-purified from non-adherent as described (Thomson et al., 1987) and 5×10^6 cells/well were cultured in 6-well plates containing 0.5 µg/mL immobilized (plastic-bound) 2C11 mAb (eBioscience).

Stimulation ± treatment with test compounds was simultaneous and consisted of a 48-hour incubation with 0.5 µM of the CD45 allosteric inhibitors. Cells were collected and whole cell lysates processed for Western blotting. Primary antibodies were monoclonal anti-pLck Y393 (Sab), anti-pZap-70 Y319 (Cell Signaling), anti-pErk (Cedarlane), and anti-α-actin (Sigma) as standard loading control. Immunoblots were developed by chemiluminescence and quantification was performed via densitometry analysis.

Quantification of Interleukin-2 secretion

Supernatant from cells stimulated ± treatment in 6 well plates for 48 hours was assayed via ELISA (Ready-Set-Go Mouse IL-2 ELISA Kit, eBioscience) following manufacturer's instructions. Optical density was read at 450 nm, and a standard curve of IL-2 was used for quantification. All assays were replicated at least 10 independent times with splenocytes from different mice, and each independent assay was the average of n=3 wells.

Cell viability assays

For all cell lines, a pre-determined number of cells were plated to achieve logarithmic growth in untreated wells. Jurkat (10,000 cells/well), J45.01 (10,000 cells/well), EL4

(6,000 cells/well), KB (10,000 cells/well), and HEK293 (4,000 cells/well) were plated in 96-well plates and treated for 24 hours as indicated in the text. Cell viability was quantified using the tetrazolium salt reagent 4-[4,5-dimethylthiazol-2-yl]-2,5-diphenyltetrazolium bromide (MTT; Sigma). Optical density readings of MTT were measured spectrophotometrically. For cell viability measuring trypan blue exclusion, cell suspensions were prepared and immediately counted under microscope.

Generation of CD45 mutants

E. coli DH5α strain was used for production and expression of recombinant mutant CD45 D1-D2 domains. The pGEX-2TK plasmid expressing CD45 gene and encoding ampicillin resistance was used as a template for mutagenesis. Primers overlapping the desired mutation region with a single or dual base pair mismatch were purchased from Integrated DNA Technologies (IDT). The mutagenic oligodeoxyribonucleotides were 5'-CTT TTA TAA TGA GCT ACT GGA TAC CTG AAG TGA TGA TTG -3' (K1003I), 5'- CTT TTA TAA TGA GCT ACT GGG CAC CTG AAG TG -3' (K1003A), 5'- GGT AGT GGA TAT TTT TCA GGG GGT AAA AGC TCT AC -3' (V1175G), and 5'- GGT AGT GGA TAT TTT TCA GGC GGT AAA AGC TCT AC -3' (V1175A). Mutations were introduced using the QuikChange Site-Directed Mutagenesis Kit (Stratagene, USA). DNA was purified (EZNA Mini-Prep Kit; Omega, USA) from Ampicillin-resistant colonies and was sequenced (McGill University and Genome Quebec Innovation Centre). The desired colonies were grown, harvested, and lysed in 20 mM HEPES-KOH pH 8.0, 500 mM NaCl, 0.1 mM EDTA, 5mM DTT and 1 mg/mL protease inhibitors. After sonication in Triton-X buffer, CD45-GST proteins were purified using Glutathione

13

Sepharose 4B beads and eluted in 50 mM Tris-HCl pH 8.0, 5mM DTT and 10 mM reduced glutathione.

Circular Dichroism (CD)

The CD Spectra of cytoplasmic CD45 D1-D2 (Enzo Lifesciences) and LAR D1-D2 (purified *in house*, GST-tagged) were studied. LAR D1-D2 is the specificity control, because the compounds do not inhibit LAR activity *in vitro*. CD45 or LAR proteins were at a final concentration of 0.04 mg/mL in 10 mM Tris buffer, pH 7.0 (adjusted with H_3PO_4). Compound **211** and **57p** were added at a concentration of 0.01 mg/mL (an approximate molar PTP:compound stoichiometry of 1:40). Phosphatases and compounds were allowed to interact in solution for ~30 minutes before measuring the CD spectra in a Chirascan spectropolarimeter (Applied Photophysics). CD spectra were recorded at 0.5 nm intervals from 180 to 280 nm at 25°C. Baseline spectrum of buffer was auto-subtracted from all samples, and the spectrum of **211** or **57p** compound alone was subtracted from the respective sample CD45 + compound. The spectra shown are representative of four independent assays. Intentional denaturation of CD45, by incubation of the same samples at 70°C for 15 minutes, was done as a control.

***In vivo* immunosuppression**

All animal protocols were approved by IACUC. Six-week old female C57/BL6 mice (Harlan Laboratory, Montreal, Canada) were used. To induce the delayed-type hypersensitivity (DTH) reaction, mice were first "primed" by 1X intraperitoneal (100 μg) and 1x subcutaneous (10 μg) injections of ovalbumin (OVA) antigen in saline. Twelve days later the mice were challenged in the right footpad with 1 μg OVA in saline, while the left footpad of each mouse was unchallenged and was used as internal control. Mice

14

were randomized and divided into four groups (n=4 each) A, B, C, and D that received drug or control treatments by 1X intraperitoneal injection. Group A is the vehicle control. Group B received 3 mg/kg **211** <1 hour after footpad antigen challenge (day 0). Group C received 3 mg/kg **211** three days after footpad antigen challenge (day 3), after initial signs of inflammation were observed. Group D remained an untreated control group until day 6, at the time of maximal footpad swelling, and at this time the mice received 3 mg/kg **211**. Right and left footpad thickness was measured at days 6-9 after footpad antigen challenge, using an electronic caliper, with the mice under mild isofluorane anesthesia. For quantification, the difference in R/L footpad thickness was calculated in each mouse, and the individual differences were pooled for each group ± sem (n=4 mice per group).

Mouse footpad section preparation and staining

Mice were sacrificed on day 9 post-challenge and feet were removed and stored at 4ºC in 4% para-formaldehyde/PBS solution. Samples were then fixed in 10% neutral buffered formalin for 48 hours, and decalcified in 6% HCl for 48 hours, and embedded in paraffin. Sections (4 µm) on SuperFrost/Plus slides (Fisher) were dried and deparaffinized in xylene and rehydrated through graded alcohols to water. Sections were stained with hematoxylin and eosin (H&E) to visualize the infiltration of immune cells in the footpad region (Gill Method, Fisher). Sections were analyzed by conventional light microscopy, and pictures were taken at 10x magnification.

Results

Identification and *in vitro* validation of hit CD45 inhibitors

The D1 and D2 domains of CD45 are joined by a flexible four amino acid linker, and several residues from each domain contribute to a stable interaction between the two. The interface forms a pocket comprising D1 and D2 as the walls, and the linker as the base (Figure 1A). We hypothesized that a small molecule might interact with a binding groove at this crevice. We screened a 120,000-compound subset of the NCI database (release 3) by *in silico* virtual docking of the compounds within the region defined by the box enclosing the D1-D2 interface (Figure 1B).

The screen identified ~200 potential binders having a predicted binding free energy of -7.5 kcal/mol or better, and these were selected for further evaluation by visual inspection of the binding mode. From these, we selected 84 compounds interacting with both the D1 and D2 domains of CD45, and whose chemical compositions satisfied the Lipinksi rule of five for drug-like properties. Compounds were procured and tested against CD45 in an *in vitro* phosphatase assay.

Compounds coded as **28p** and **37p** (Figure S-1A) inhibited, in a dose-dependent manner, the ability of CD45 to dephosphorylate pp60-Src peptide. Compounds **28p** and **37p** have IC_{50} values of 4.6 µM and 1.1 µM respectively (Figure 2A). Eighty-two other compounds did not inhibit CD45 at concentrations >50 µM and were not pursued.

These "hits" were docked at a pocket of CD45 formed by the interface of D1-D2 and the linker that joins these domains. Residues from D1 and D2 form hydrogen bonds and hydrophobic contacts with compounds **28p** or **37p**. For both inhibitors, the D2 domain contributes the majority of predicted contacts (see Supplemental Figures S-1B and S-1C).

16

CD45 selectivity of the inhibitors

The "hit" CD45 inhibitors **28p** and **37p** were tested against a panel of protein tyrosine phosphatases that include LAR, PTP1B, PTP Sigma, SHP-1, and MKPX. These PTPs were chosen because they bear structural similarity to CD45, and the tandem phosphatase domains D1 and D2 are highly conserved among the receptor-like proteins CD45, LAR and PTP Sigma. The IC_{50} data are summarized in Table 1.

28p was a broad inhibitor of all PTPs tested, and in fact it was a more potent inhibitor of PTP1B and SHP-1 than of CD45. **37p** was highly selective for CD45 phosphatase. Amongst the PTPs tested, the only other effect detected was on PTP1B, but with a significant 15-fold difference in IC_{50}. As a control, we show one compound **57p**,also predicted to dock near the CD45 D1-D2 interface by the *in silico* screen, but which did not inhibit any of the PTPs on the panel. Supplemental Figure S-2 shows the inhibition profiles of **28p** versus a PTP panel, and of **37p** versus PTP1B.

The different binding modes predicted for **37p** and **28p** provide a possible explanation for selectivity by **37p** and the lack of selectivity by **28p**. Strong **28p** interactions with the D1 domain may be sufficient to cause inhibition of PTP1B and SHP-1 which lack a D2 domain, making **28p** non-selective. In contrast, **37p** causes poor inhibition of PTPs lacking a D2 domain (e.g. constructs of PTPs LAR and Sigma expressing both domains were tested in counter-assays).

For further validation, the activity of all control PTPs were tested using two different substrates, yielding similar results: pNPP (data shown in Table 1, see supplemental for details) and DIFMUP (supplemental Figure S-2C). In addition, the activity of control

17

LAR was also tested using an insulin receptor-derived phospho-peptide, also yielding similar results (data not shown).

Because pNPP and DIFMUP are not good substrates *in vitro* for CD45, they were not used for this enzyme. Instead, CD45 inhibition was tested independently against two different phospho-peptides representing the cognate Src substrates at positions pY-527 (data shown in Table 1) and pY-416 (see Figure 3 below).

Based on CD45 selectivity, we chose **37p** for developing second-generation agents.

Hit-to-lead generation

The **37p** molecule was cut at two locations, and by rational design we determined that the remaining central phenyl ring should be derivatized with substituents at the ortho-, meta- and para- positions. Twenty-nine analogs of **37p** were thus purchased and tested in the *in vitro* phosphatase assays. Five analogs are shown, coded **210**, **211**, **214**, **215**, and **216**. (Figure 2B). They are potent and selective CD45 inhibitors, with improved inhibition of CD45 by two-fold to four-fold over the parent compound **37p** (Figure 2C), reaching nanomolar IC$_{50}$. With regards to selectivity, these five analogs retained selectivity against CD45 (Table 1) and did not significantly inhibit other PTPs at 50 µM (the highest dose tested). Thus, compounds **210**, **211**, **214**, **215**, and **216** are smaller and more potent than the parent, and are highly selective for CD45.

Analog **211** was selected as a lead compound due to its high potency, selectivity, stability, and membrane permeability predicted *in silico*. Because **211** was considered a lead, additional selectivity controls **were completed** against PTPs PTPN22 (the catalytic domain PEP and the full-length PTPN22) that plays a role in T cell signaling, as well as

18

its family member PEST. Compound **211** had no effect on the *in vitro* phosphatase activity of these enzymes (Table S-2).

Allosteric binding site of 211 on CD45 phosphatase

The *in silico* model of the binding of **211** on the CD45 pocket is shown (Figure 2D). The compound is anchored at one end by a hydrogen bond between its acetyl carbonyl and the Ser1163 side chain hydroxyl group. The acetyl methyl packs against a hydrophobic surface formed by the side chains of Val1175 and Leu1160. At the opposite end, one of the naphthoquinone oxygens forms a hydrogen bond with the side chain ammonium of Lys1003. The increased potency of **211** over **37p** may be partly due to its having three times fewer rotatable bonds, resulting in a lower entropic cost upon binding.

To validate the predicted **211** binding model, we generated mutant CD45 proteins with substitutions affecting two of the predicted binding sites. Lys1003 was predicted to form a tight hydrogen bond with the carbonyl group of the core structure of **211** (Figure 2D), while Val1175 contributes to hydrophobic interactions with the side-chain aromatic ring of **211**. If a mutant CD45 retains phosphatase *in vitro* catalytic activity, but **211** can not inhibit it, this can be interpreted as a failure of **211** to bind at the mutant pocket. Thus, wild type Lys1003 was mutated to Ile or Ala, and wild type Val1175 was mutated to Gly or Ala, for a total of four point mutants.

The wild type and mutant CD45 intracellular D1-D2 domain proteins were purified and used in phosphatase *in vitro* assays ± **211** (Figure 2E). We first established that mutant forms of CD45 have the same level of phosphatase activity as wild-type enzyme (see Supplemental Figure S-3 for phosphatase activity). Compound **211** did not inhibit CD45 mutants K1003A and V1175A, but inhibited wild type CD45, at the two

19

concentrations tested. In addition, compound **211** inhibited mutants K1003I and V1175G

at a significantly reduced rate. As a control, we observed strong inhibition of both wild-

type and mutant CD45 when using competitive CD45 inhibitor RWJ-60475 (Beers et al.,

1997). This confirms that mutated CD45 behaves similarly to wild type CD45, and taken

together, validates the region encompassing the K1003 and V1175 residues as the

orthosteric binding site for **211**.

We postulated that an allosteric inhibitor binding at that site could influence CD45

phosphatase activity through conformational changes. We measured the circular

dichroism spectra of CD45 with and without **211** (Supplemental Figure S-4A). When **211**

is co-incubated with CD45 it appears that there is a dramatic loss of secondary structure,

akin to an unfolding of the protein. This effect was not observed in the presence of non-

inhibitory compound **57p**, and when LAR phosphatase was co-incubated with **211** there

was no change in secondary structure in this control protein (Supplemental Figure S-4B).

Together, the data in Figure 2 validate that functional inhibition by **211** requires a

structure near the CD45 D1-D2 linker region, which is outside the orthosteric site. The

circular dichroism data suggest a conformational change as a possible cause for reduced

CD45 activity.

Non-competitive and irreversible mechanism of inhibition

Docking, modeling and site-directed mutagenesis data suggest an allosteric pocket far

from the orthosteric substrate binding and catalytic site. To address the mechanism of

action, we studied the inhibition of CD45 by **211** at three different concentrations of

phospho-peptide substrate.

The inhibitor and substrate were added simultaneously to CD45 enzyme. CD45

activity was measured after 20 minutes incubation of the indicated four different

concentrations of **211** and the indicated three different concentrations of pp60-src

substrate. A double-reciprocal Lineweaver-Burk analysis of reaction velocity (1/Vo)

versus substrate concentration (1/So) showed that all lines intersect at a common –Km

value. These data indicate a non-competitive mode of inhibition (Figure 3A).

To further characterize the mechanism of inhibition, potential reversibility of the

inhibition was studied *in vitro versus* two src-derived phospho-peptide substrates. The

inhibition of CD45 was plotted over time, up to 120 minutes (reaction plateaus after 20

minutes when substrate is depleted). If the inhibition were reversible one would expect

the phosphatase reaction to proceed slowly over time. However, the **211**-treated CD45

shows an early plateau indicating an irreversible mechanism of inhibition (Figure 3B, and

3C). In a permutation of this assay, addition of more substrate to the reaction after 20

minutes showed that while untreated CD45 remains active, the **211**–treated CD45 is not

active.

It is worth noting that **211** is very effective at preventing CD45 dephosphorylation of

pY-527-peptide substrate (~80% inhibition at Vmax, Figure 3B) and it is less effective at

preventing CD45 dephosphorylation of the pY-416-peptide substrate (~35% inhibition at

Vmax, Figure 3C). This observation further supports an allosteric mechanism of action,

because poisoning the catalytic site of CD45 prevents activity equally at any substrate.

These data allows us to make predictions about the cellular consequences of

CD45 inhibition. CD45 dephosphorylates both the regulatory C-terminal tyrosine (Y505)

and the autocatalytic tyrosine (in human Lck it is position Y394, in mouse Lck it is

21

position Y393). Functional CD45 thus creates a state of equilibrium for Lck molecules that allows for a primed Lck response when the T cell receptor is engaged. Preferential inhibition of the removal of the inhibitory tyrosine, by **211**, can shift the pool of Lck molecules towards the inactive state. The phosphorylated C-terminal Y505 of Lck interacts intramolecularly with its own SH2 domain, thus sequestering Y393. In this conformation, trans-phosphorylation of Y393 is not possible and Lck remains inactive. Thus, we can predict that the reduced pool of resting state Lck would result in diminished activation of the T cell signaling pathway in the presence of CD45 inhibitor **211**.

CD45 inhibition by 211 does not involve oxidative mechanisms

Irreversible inhibition by **211** could suggest a mechanism of oxidation of one or more cysteine residues in CD45. There is a precedent in 1,2-napthoquinone (1,2-NQ) that inhibits CD45 through oxidation in a substrate-reversible manner (Urbanek et al., 2001). However, our data indicates that **211** inhibits CD45 non-competitively with respect to substrate (see Figure 3A). 1,2-NQ is also an irreversible inhibitor of PTP1b through covalent modification of cysteines (Iwamoto et al., 2007).

Hence, we studied whether **211** could modify free cysteines of CD45 or PTP1b, and 1,2-NQ was used as a positive control. Assays employing DTNB substrate quantified the free sulfhydryl groups (SH) in the proteins with and without compound treatment. Treatment conditions, times of incubation, and protein-compound stoichiometry replicated the conditions used in the PTPase functional assays, except that DTT was omitted because it prevents or reverses oxidative mechanisms (Iwamoto et al., 2007; Urbanek et al., 2001).

211 did not diminish free -SH in CD45 or in PTP1b (Figure 3D). The positive control

1,2-NQ diminished free -SH in PTP1b by ~85% and did not detectably affect free -SH in CD45 (Figure 3D). Note that under these assay conditions **211** inhibits the activity of CD45 *selectively* by ~80% (even in the presence of freshly added reducing agent -2 mM DTT-); whereas 1,2-NQ inhibits both CD45 and PTP1b (and its efficacy on PTP1b is affected by the presence of DTT).

Together, the data indicate that **211** (i) inhibits CD45 selectively over several other PTPases, (ii) has an allosteric site that requires residues at the linker domain of D1-D2, (iii) alters the structure of intracellular CD45, (iv) is irreversible, (v) is non-competitive, and (vi) does not inhibit by way of free –SH chemical modification.

Cellular CD45 activity is inhibited by 211

To study whether cellular CD45 is a target of **211**, we studied changes in the phosphorylation of Lck because it is a substrate of CD45. We studied Jurkat T cells and utilized the CD45-negative variant of Jurkat, called J45.01, as a control. J45.01 exhibit impaired TCR signalling and are hyper-phosphorylated at the Tyr505 position of Lck (Koretzky et al., 1991). Each of these two cell lines were treated for 24 hours with vehicle control or **211** at 0.5 µM, and lysates were probed by Western Blot for various forms of Lck (Figure 4) and quantified by densitometry using total Zap-70 as control.

In Jurkat cells (human, hence Lck pY394 position is used), treatment with **211** caused a ~50% increase in Lck pY394 compared to untreated cells (significant $p < 0.05$; see Figure 4D for quantification). However, in J45.01 cells, treatment with **211** caused no change in Lck pY394 (Figure 4A). In both Jurkat and J45.01 cells, treatment with **211** caused no change in baseline Lck pY-505 (Figure 4B) or in total Lck (Figure 4C).

Because CD45 normally dephosphorylates the Lck pY-394 position, it is expected that a CD45 inhibitor would increase Lck pY-394 phosphorylation above baseline levels. Thus, quantifying the phosphorylation of Lck as a surrogate assay for CD45 activity, we conclude that **211** inhibits the function of CD45. Based on the data from J45.01 cells (which express many PTPases) we infer that CD45 expression is required to detect changes in Lck pY-394.

Non-specific toxicity by CD45 inhibitors was excluded by assays measuring metabolic activity in lymphoid cells (Jurkat, J45.01 cells) as well as non-lymphoid cells that do not express CD45 (KB and HEK293 cells). After 24 hours of culture with 0.5 μM CD45 inhibitors (the concentration used for biochemical assays) the percent of cell viability was not affected (Supplemental Table S-1).

CD45 inhibitors diminish T Cell Receptor signalling in activated splenocytes

Studies of T-cell receptor signalling were extended in biochemical and biological assays using semi-purified primary T cells. Freshly isolated mouse T cells were stimulated by cross-linking anti-CD3 antibody 2C11 for 48 hours ± CD45 inhibitors **37p** and its analog **211**, each at 0.5 μM. Whole cell lysates were processed in western blots probed with antibodies against Lck pY-393, Zap-70 pY-319, and p-MAPK. These proteins are phosphorylated following a signal from the TCR.

The TCR-stimulated cultures had significant induction of Lck pY-393, Zap-70 pY-319, and p-MAPK (Figure 5A), compared to the control non-stimulated culture. Treatment with **211** causes a reduction of 40-50% in TCR-mediated activation (Figure 5B). Thus, these compounds affect signalling through the TCR, likely because they interfere with CD45 function. As a further readout, we measured IL-2 protein released in

24

the supernatants. As measured by quantitative ELISA tests, IL-2 levels were significantly

reduced in the drug-treated groups compared to the vehicle-treated group (Figure 5C). In

baseline controls, cells not activated by TCR cross-linking did not produce detectable IL-

2, indicating that this is a reliable readout of TCR (and CD45)-mediated activation.

Inhibition of Lck pY-393 and IL-2 production by compound **211** are consistent with each

other. However, inhibition by **37p** was less pronounced than anticipated from the *in vitro*

assays, likely because it is not stable in aqueous solutions for longer than 12 hours (data

not shown).

To rule out a direct cytotoxic effect, cell viability (trypan blue exclusion) and

metabolic activity (MTT assays) were tested in primary splenocytes treated with CD45

inhibitors. These assays were done using the same culture and activation conditions used

for the biochemical and bioassays above. At the relevant concentration of 0.5 μM **211**,

the trypan blue exclusion method revealed no changes in the ratio of live-to-dead cells

after treatment, compared to untreated control (Figure 5E). However, the MTT assays

revealed that there was ~40% less metabolic activity in the **211**-treated, TCR-stimulated

splenocytes (Figure 5D). Thus, it appears that CD45 inhibitors do not compromise cell

integrity, yet they prevent TCR-mediated activation and therefore prevent an increase of

the cellular metabolic rate. Reduced metabolic rate correlates with decreased IL-2

production and inhibition of T-cell signalling pathways.

We also investigated the ability of CD45 inhibitor **211** to influence Lck

phosphorylation in resting splenocytes treated with 0.5 μM compound for 48 hours, but

without TCR cross-linking. Lck pY-393 and pY-505 did not change after **211**-treatment

(see Supplemental Figure S5). This was expected because there is no TCR signal driving

the activation and proliferation of these cells, hence CD45 function is not absolutely required, and CD45 inhibition by **211** should not impact on the signaling pathway.

Taken together, the data show that a potentially allosteric CD45 inhibitor causes a chemical knockdown of CD45 function, and diminishes TCR-dependent activation and signalling.

A CD45 inhibitor is immunosuppressive *in vivo*

Compound **211** was selected for studies *in vivo*, in wild type C57/BL6 mice. A dose-escalation study of a single intraperitoneal injection for compound **211** up to the maximum dose tested of 12 mg/kg, showed that it was well tolerated with the only undesirable side-effect being ~25% neutropenia after 24 hours.

A dose of 3 mg/kg caused a ~50% decrease in lymphocytes without significant neutropenia, no observable adverse side effects in behaviour, no change in creatinine or amylase levels, or in the numbers of red blood cells and platelets.

We tested compound **211** at a dose of 3 mg/kg in a footpad model of delayed type hypersensitivity (DTH) in wild type C57/BL6 mice. In this model we detect signs of increased footpad thickness, redness, and inflammation at day 3 after challenge; with maximal footpad thickness at day 6 post-challenge. Compound **211** (3 mg/kg single dose) was injected intraperitoneally within 1 hour of footpad challenge (day 0, group B) or at day 3 after footpad challenge (day 3, Group C) (flow-chart Figure 6A).

In Group B, injected within an hour of challenge, there was only slight inflammation in 1/4 mice at day 3, and no progression to full DTH in any of the mice at day 6 post-challenge (Figure 6B). These data indicate that systemic inhibition of CD45 at the time of

26

footpad insult results in a block of DTH induction and that the efficacy of inhibition of CD45 can be long–lasting.

In Group C, injected with **211** at day 3 post-challenge, inhibition of DTH was achieved even though drug was delivered *after* early onset of inflammation. Quantification done at day 6 post-challenge showed that this group had an almost complete normalization of footpad thickness, compared to control (group A) and untreated mice (group D) (Figure 6B). These data indicate that the CD45 inhibitor is effective at preventing DTH when administered systemically at the onset of inflammation.

When compound **211** was injected at day 6 after challenge (group D), a time when inflammation is maximal, there was no significant reduction of footpad thickness over the following three days (e.g. until day 9 post-challenge). Thus, while the CD45 inhibitor might prevent T-cell mediated inflamation, it does not clear the existing edema in the footpad.

Staining of paraffin-embedded footpad sections with H&E confirmed the presence of greater infiltration of cells in the vehicle-treated control (group A) compared to groups B or C, which had received 3 mg/kg **211** at day 0 and day 3 respectively (Supplemental Figure S-6). A further comparison of the right foot (challenged, untreated) versus the left foot (naïve, untreated) of a mouse from group A shows the degree of cellular infiltration. The infiltrating cells are presumed to be lymphoid based on morphology. Thus, the inflammation after ovalbumin challenge was likely mediated by an immune response, which is suppressed by CD45 inhibitor **211**.

27

Discussion

This work provides evidence of an allosteric site in CD45, where a non-competitive small molecule can bind, and cause inhibition of the CD45 protein tyrosine phosphatase activity. The inhibitors were effective immunomodulators *ex vivo* and *in vivo*, and therefore they may be interesting lead compounds for therapeutic programs. Importantly, similar approaches can be used to target the D1-linker-D2 interface of other PTPs.

Binding at a non-orthosteric pocket, and allosteric mechanisms

Molecular docking and site directed mutagenesis suggests that the CD45 inhibitors bind in a pocket near the interface between the D1 and D2 domains, adjacent to the linker region. Hit compounds **28p** and **37p** were predicted to dock at this allosteric site. **37p** exhibits selectivity towards CD45 over similarly structured PTPs such as LAR, and is smaller and more compact than the non-selective **28p.** A compound derived from **37p**, compound **211**, was also modeled to bind in the D1-D2 pocket.

A key interaction for **211** was predicted to be at CD45 Lys1003 through a hydrogen bond with the "core" naphthoquinone moiety of **211** and **37p**. Furthermore, the "non-core" portion of **211**, an anilino-phenyl ring with an acetyl side group, was also predicted to interact with CD45 through hydrophobic interactions with Leu1160 and Val1175, as well as a second hydrogen-bond with Ser1163. These predictions are consistent with the site-directed mutagenesis data. Mutation of Lys1003 and Val1175 did not compromise CD45 phosphatase activity but abolished the capacity of **211** to inhibit CD45 activity.

Site-directed mutagenesis strongly indicate an allosteric mechanism of action. Mutated serine and valine residues prevented **211**, but not competitive inhibitor RWJ, from inhibiting CD45 phosphatase activity. Interestingly, the *in vitro* phosphatase activity

of the mutant CD45 enzymes was equivalent to that of wild type CD45; suggesting that these residues are not critical to CD45 activity. However, the CD45 residues that were mutated are required for **211**-induced inhibition.

It is likely that these residues allow **211** to interact with and reposition the D2 domain, which in turn impacts on the D1 domain that contains the catalytic region. This is supported by the change in conformation noted in the CD experiments, where **211** caused significant changes to the alpha-helicity of the CD45 intracellular domain but did not affect the overall structure of the intracellular domain of LAR or LAR activity *in vitro*.

Together, the data indicate that the inhibitor inflicts a conformational change upon CD45, potentially unfolding the protein. There are precedents where an allosteric inhibitor irreversibly destabilizes an enzyme via a non-oxidative mechanism (Dominguez et al., ; Piver et al., 2001; Ucar et al., 2005).

High potency and selectivity at inhibiting CD45 signaling in T cells

It is encouraging that the *in vitro* data correlates with the cell-based biochemical and biological data. **211** inhibition of CD45 caused a differential effect upon the two CD45 substrates. There was increased Lck pY-393, an indication that CD45 function is inhibited. On the other hand, there were no changes in the steady-state Lck pY-505, which is also dephosphorylated by CD45.

This was a surprising result, as we expected both pY-393 and pY-505 to increase in CD45-inhibited T cells. However, our observation is consistent with reports that only high CD45 activity can dephosphorylate Lck pY-393 while low CD45 activity is sufficient to dephosphorylate Lck pY-505 (McNeill et al., 2007). Thus, it is possible that

after pharmacological inhibition of CD45 the pY-505 remains in a steady state but pY-393 levels are increased.

In resting primary T cells, there are low to undetectable Lck pY-393 but there are significant levels of Lck pY-505. Stimulation with TCR cross-linking results in a time-dependent increase in Lck pY-393 and no detectable changes in the steady state of Lck pY-505. Thus, inhibition of CD45 during stimulation via TCR results in the prevention of the time-dependent increase in Lck pY-393; without significant alterations to the steady state of Lck pY-505. These events result in the inactivation of Lck, as demonstrated by downstream readouts (e.g. p-Zap-70, p-MAPK, IL-2 production are reduced by CD45 inhibitors).

These data are consistent with the view that CD45 functions as a rheostat to keep Lck in a 'primed' state, ready for activation (Hermiston et al., 2003). The allosteric CD45 inhibitors reduce CD45 activity and the pool of Lck that is capable of becoming activated. Under TCR-mediated stimulation, if removal of p-Y505 is inefficient, the Lck molecule is commonly referred to as "inactive", because Y393 is inaccessible for auto-phosphorylation (Amrein et al., 1993). This results in hypo-phosphorylation of Y393 with minimal effects detected on the steady state phosphorylation of Y505. Poor Lck activation extends to inefficient recruitment of Zap-70 to the CD3 ζ-chain and poor Zap-70 pY-319. Downstream of this, CD45 inhibitors reduce the amount of p-Erk, indicating effects upon cellular proliferation (Crawley et al., 1997), decrease IL-2 production, and reduce metabolic activity in the T cells.

Substrate specificity

Compound **211** is a selective inhibitor of CD45, and does not affect several related

PTPases. Notably, **211** also has some degree of substrate specificity when two pp60-Src phosphopeptides were tested. The dephosphorylation of the negative regulatory pp60-Src pTyr is inhibited by ~80%. The dephosphorylation of the autocatalytic activating pp60-Src pTyr is inhibited by ~35%. To our knowledge, this is the first report of a differential inhibition of these substrates.

Immunosuppression *in vivo*

The DTH reaction to ovalbumin was inhibited in footpad-challenged mice by treating them with a single dose of 3 mg/kg **211**. This was accomplished in a therapeutic paradigm administering **211** after antigen challenge, and after slight inflammation had already set in. However, there was no suppression of the signs of edema when the inflammatory response was well-established, likely because T cell activation is not relevant at this stage of pathology (Askenase and Van Loverent, 1983).

DTH prevention is likely due to the inhibition of T cell activation during antigen challenge, and not due to the apoptosis of T cells. The dose of 3 mg/kg did reduce circulating lymphocytes by ~50%, but given that the *in vivo* data was collected six days after the single injection of **211**, circulating lymphocytes had ample time to recover from depletion. At day 6, inhibition of footpad inflammation was near 100%, which we interpret as the complete blockage of T cell activation.

Conclusion

In this work, we have identified and validated a novel binding site for inhibitors on CD45 phosphatase intracellular domain, identified inhibitors *in vitro*, and improved upon their potency for CD45 inhibition via chemical modification. A lead allosteric CD45 inhibitor suppresses splenocyte activation and inhibits the immune response *in vivo*.

31

Together, the findings bode well for potential therapeutic applications of allosteric CD45 inhibitors. In particular, CD45 inhibitors may be used as immunosuppressive agents relevant in the treatment of T-cell or B-cell mediated autoimmune diseases, preventing organ transplant rejection, and in certain forms of leukemia or lymphoma. The targeting of an allosteric site on CD45 may be expanded to target similar domains of other PTPs.

Acknowledgments

Authorship contribution

Participated in research design: Perron, Saragovi.

Conducted experiments: Perron, Chowdhury, Aubry, Saragovi.

Contributed new reagents or analytic tools: Purisima.

Performed data analysis: Perron, Chowdhury, Aubert, Tremblay, Saragovi.

Wrote or contributed to the writing of the manuscript: Perron, Chowdhury, Tremblay, Saragovi.

References

Alexander DR (2000) The CD45 tyrosine phosphatase: a positive and negative regulator of immune cell function. *Semin Immunol* **12**(4):349-359.

Amrein KE, Panholzer B, Flint NA, Bannwarth W and Burn P (1993) The Src homology 2 domain of the protein-tyrosine kinase p56lck mediates both intermolecular and intramolecular interactions. *Proc Natl Acad Sci U S A* **90**(21):10285-10289.

Askenase PW and Van Loverent H (1983) Delayed-type hypersensitivity: activation of mast cells by antigen-specific T-cell factors initiates the cascade of cellular interactions. *Immunology Today* **4**(9):259-264.

Beers SA, Malloy EA, Wu W, Wachter MP, Gunnia U, Cavender D, Harris C, Davis J, Brosius R, Pellegrino-Gensey JL and Siekierka J (1997) Nitroarylhydroxymethylphosphonic acids as inhibitors of CD45. *Bioorg Med Chem* **5**(12):2203-2211.

Bhat S and Purisima EO (2006) Molecular surface generation using a variable-radius solvent probe. *Proteins* **62**(1):244-261.

Blaskovich MA (2009) Drug discovery and protein tyrosine phosphatases. *Curr Med Chem* **16**(17):2095-2176.

Case DA, Cheatham TE, 3rd, Darden T, Gohlke H, Luo R, Merz KM, Jr., Onufriev A, Simmerling C, Wang B and Woods RJ (2005) The Amber biomolecular simulation programs. *J Comput Chem* **26**(16):1668-1688.

Crawley JB, Rawlinson L, Lali FV, Page TH, Saklatvala J and Foxwell BM (1997) T cell proliferation in response to interleukins 2 and 7 requires p38MAP kinase activation. *J Biol Chem* **272**(23):15023-15027.

Cui Q, Sulea T, Schrag JD, Munger C, Hung MN, Naim M, Cygler M and Purisima EO (2008) Molecular dynamics-solvated interaction energy studies of protein-protein interactions: the MP1-p14 scaffolding complex. *J Mol Biol* **379**(4):787-802.

D'Oro U, Sakaguchi K, Appella E and Ashwell JD (1996) Mutational analysis of Lck in CD45-negative T cells: dominant role of tyrosine 394 phosphorylation in kinase activity. *Mol Cell Biol* **16**(9):4996-5003.

Dominguez JM, Fuertes A, Orozco L, del Monte-Millan M, Delgado E and Medina M Evidence for irreversible inhibition of glycogen synthase kinase-3beta by tideglusib. *J Biol Chem* **287**(2):893-904.

Felberg J and Johnson P (1998) Characterization of recombinant CD45 cytoplasmic domain proteins. Evidence for intramolecular and intermolecular interactions. *J Biol Chem* **273**(28):17839-17845.

Glover NR and Tracey AS (2000) The phosphatase domains of LAR, CD45, and PTP1B: structural correlations with peptide-based inhibitors. *Biochem Cell Biol* **78**(1):39-50.

Greer SF, Wang Y, Raman C and Justement LB (2001) CD45 function is regulated by an acidic 19-amino acid insert in domain II that serves as a binding and phosphoacceptor site for casein kinase 2. *J Immunol* **166**(12):7208-7218.

Hamaguchi T, Takahashi A, Manaka A, Sato M and Osada H (2001) TU-572, a potent and selective CD45 inhibitor, suppresses IgE-mediated anaphylaxis and murine contact hypersensitivity reactions. *Int Arch Allergy Immunol* **126**(4):318-324.

Hardy JA and Wells JA (2004) Searching for new allosteric sites in enzymes. *Curr Opin Struct Biol* **14**(6):706-715.

Hermiston ML, Xu Z and Weiss A (2003) CD45: a critical regulator of signaling thresholds in immune cells. *Annu Rev Immunol* **21**:107-137.

Irwin JJ and Shoichet BK (2005) ZINC--a free database of commercially available compounds for virtual screening. *J Chem Inf Model* **45**(1):177-182.

Iwamoto N, Sumi D, Ishii T, Uchida K, Cho AK, Froines JR and Kumagai Y (2007) Chemical knockdown of protein-tyrosine phosphatase 1B by 1,2-naphthoquinone through covalent modification causes persistent transactivation of epidermal growth factor receptor. *J Biol Chem* **282**(46):33396-33404.

Jacobsen M, Schweer D, Ziegler A, Gaber R, Schock S, Schwinzer R, Wonigeit K, Lindert RB, Kantarci O, Schaefer-Klein J, Schipper HI, Oertel WH, Heidenreich F, Weinshenker BG, Sommer N and Hemmer B (2000) A point mutation in PTPRC is associated with the development of multiple sclerosis. *Nat Genet* **26**(4):495-499.

Jakalian A, Jack DB and Bayly CI (2002) Fast, efficient generation of high-quality atomic charges. AM1-BCC model: II. Parameterization and validation. *J Comput Chem* **23**(16):1623-1641.

Justement LB (1997) The role of CD45 in signal transduction. *Adv Immunol* **66**:1-65.

Kashio N, Matsumoto W, Parker S and Rothstein DM (1998) The second domain of the CD45 protein tyrosine phosphatase is critical for interleukin-2 secretion and substrate recruitment of TCR-zeta in vivo. *J Biol Chem* **273**(50):33856-33863.

Koretzky GA, Picus J, Schultz T and Weiss A (1991) Tyrosine phosphatase CD45 is required for T-cell antigen receptor and CD2-mediated activation of a protein tyrosine kinase and interleukin 2 production. *Proc Natl Acad Sci U S A* **88**(6):2037-2041.

Kung C, Pingel JT, Heikinheimo M, Klemola T, Varkila K, Yoo LI, Vuopala K, Poyhonen M, Uhari M, Rogers M, Speck SH, Chatila T and Thomas ML (2000) Mutations in the tyrosine phosphatase CD45 gene in a child with severe combined immunodeficiency disease. *Nat Med* **6**(3):343-345.

McNeill L, Salmond RJ, Cooper JC, Carret CK, Cassady-Cain RL, Roche-Molina M, Tandon P, Holmes N and Alexander DR (2007) The differential regulation of Lck kinase phosphorylation sites by CD45 is critical for T cell receptor signaling responses. *Immunity* **27**(3):425-437.

Naim M, Bhat S, Rankin KN, Dennis S, Chowdhury SF, Siddiqi I, Drabik P, Sulea T, Bayly CI, Jakalian A and Purisima EO (2007) Solvated interaction energy (SIE) for scoring protein-ligand binding affinities. 1. Exploring the parameter space. *J Chem Inf Model* **47**(1):122-133.

Nam HJ, Poy F, Saito H and Frederick CA (2005) Structural basis for the function and regulation of the receptor protein tyrosine phosphatase CD45. *J Exp Med* **201**(3):441-452.

Pingel JT and Thomas ML (1989) Evidence that the leukocyte-common antigen is required for antigen-induced T lymphocyte proliferation. *Cell* **58**(6):1055-1065.

Piver B, Berthou F, Dreano Y and Lucas D (2001) Inhibition of CYP3A, CYP1A and CYP2E1 activities by resveratrol and other non volatile red wine components. *Toxicol Lett* **125**(1-3):83-91.

Purisima EO (1998) Fast Summation Boundary Element Method for Calculating Solvation Free Energies of Macromolecules. *J Comput Chem* **19**:1494-1504.

Riddles PW, Blakeley RL and Zerner B (1983) Reassessment of Ellman's reagent. *Methods Enzymol* **91**:49-60.

Streuli M, Hall LR, Saga Y, Schlossman SF and Saito H (1987) Differential usage of three exons generates at least five different mRNAs encoding human leukocyte common antigens. *J Exp Med* **166**(5):1548-1566.

Streuli M, Krueger NX, Thai T, Tang M and Saito H (1990) Distinct functional roles of the two intracellular phosphatase like domains of the receptor-linked protein tyrosine phosphatases LCA and LAR. *Embo J* **9**(8):2399-2407.

Thomas ML and Brown EJ (1999) Positive and negative regulation of Src-family membrane kinases by CD45. *Immunol Today* **20**(9):406-411.

Thomson AW, Mathie IH and Sewell HF (1987) Cyclophosphamide-induced eosinophilia in the rat: concomitant changes in T-cell subsets, B cells and large granular lymphocytes within lymphoid tissues. *Immunology* **60**(3):383-388.

Trowbridge IS and Thomas ML (1994) CD45: an emerging role as a protein tyrosine phosphatase required for lymphocyte activation and development. *Annu Rev Immunol* **12**:85-116.

Ucar G, Gokhan N, Yesilada A and Bilgin AA (2005) 1-N-Substituted thiocarbamoyl-3-phenyl-5-thienyl-2-pyrazolines: a novel cholinesterase and selective monoamine oxidase B inhibitors for the treatment of Parkinson's and Alzheimer's diseases. *Neurosci Lett* **382**(3):327-331.

Urbanek RA, Suchard SJ, Steelman GB, Knappenberger KS, Sygowski LA, Veale CA and Chapdelaine MJ (2001) Potent reversible inhibitors of the protein tyrosine phosphatase CD45. *J Med Chem* **44**(11):1777-1793.

Wang Y, Guo W, Liang L and Esselman WJ (1999) Phosphorylation of CD45 by casein kinase 2. Modulation of activity and mutational analysis. *J Biol Chem* **274**(11):7454-7461.

Word JM, Lovell SC, Richardson JS and Richardson DC (1999) Asparagine and glutamine: using hydrogen atom contacts in the choice of side-chain amide orientation. *J Mol Biol* **285**(4):1735-1747.

Footnotes

This work was funded by a Proof-of-Principle grant from Canadian Institutes of Health Research to HUS and MLT.

MOL #89847

Legends for figures

Figure 1. Docking of compounds at a pocket region near the CD45 D1 D2 domain interface.

(**A**) The phosphatase active site is located at the D1 domain, bound to the CD3-ζ ITAM-1 phosphopeptide. The D1 and D2 domains are shown in green and yellow respectively. (**B**) The red box located at the pocket region near the interface between the D1 and D2 domains was the target of NCI database screening and represents the putative binding pocket of the compounds.

Figure 2. Hit-to-lead optimization and characterization of inhibitory molecules

(**A**) Hits **28p** and **37p** were tested for inhibition of CD45 phosphatase. Enzyme was pre-incubated with compound (from 5 nM to 50 μM) for 10' before addition of a synthetic phosphorylated peptide derived from the negative regulatory site of pp60-Src, and the reaction was proceeded for 20'. Data are expressed as % ± SEM of untreated control. n = 6 independent assays, each in triplicate. $r^2 > 0.85$. The structure of **37p** is shown. (**B**) Evolution of **37p** in hit-to-lead compounds. The structures of five analogs (**210**, **211**, **214**, **215**, and **216**) are shown. They are of reduced size, derivatized at the ortho-, meta- and para- positions on the aromatic ring. (**C**) Analogs were tested for inhibition of CD45 phosphatase, compared versus **37p**. Data are expressed as % of untreated control ± SEM. n = 4 independent assays, each in triplicate. $r^2 > 0.85$. (**D**) **211** was selected as the lead compound for future experiments and its binding mode near the CD45 D1-D2 interface is shown. Hydrogen bond interactions are displayed as dashed lines. (**E**) Inhibition by **211** was assayed at 1 μM and 10 μM against CD45 point mutants K1003I, K1003A, V1175G

38

and V1175A. Competitive inhibitor RWJ is a control as it inhibits all mutants. Lack of inhibition by **211** validates experimentally the binding site predicted by the *in silico* model.

Figure 3. Binding mode and reversibility of CD45 inhibitor 211

(**A**) Lineweaver-Burk analysis of **211** inhibition on CD45 phosphatase. CD45 activity was measured at varying substrate concentrations as described in Materials & Methods, at the indicated concentrations of **211**. The data is representative of three independent experiments. (**B, C**) The reversibility of **211** inhibition of CD45 was assayed by allowing the assay to proceed for 120 minutes. Substrates tested include the inhibitory c-terminal pY-527 and the autocatalytic Src phospho-substrate pY-416. (**D**) **211** does not oxidize free cysteines in CD45 or in PTP1b. A chemically related compound 1,2-naphtoquinone known to oxidize PTP1b is used as a positive control.

Figure 4. Validation of CD45 as a cellular target

Jurkat cells (CD45 +ve, expressing wild type levels of CD45) or J45.01 cells (CD45 –ve, CD45-negative Jurkat clone) were treated with 0.5 µM **211**, or untreated (control). After 24 hours, samples were immunoblotted with antibodies to (**A**) p-Lck Y394, (**B**) p-Lck Y505, or (**C**) total Lck. (**D**) Quantification of band intensity was normalized to total Zap-70. Results are displayed as a percent of the untreated control, each bar representing the mean (± SEM) of three individual experiments. (*) significant $p < 0.05$ by student's t-test.

Figure 5. Characterization of CD45 inhibitors *ex vivo*

Mouse splenocytes were stimulated with α-CD3 ± 0.5 µM CD45 inhibitors **37p** and **211**.

(**A**) Representative western blots of whole cell lysates immunoblotted with α-pLck Tyr393, α-pZap-70 Tyr319, and α-pErk 1,2 (from ten independent experiments). (**B**) Optical density quantification of phospho-Lck, phospho-Zap-70 and phospho-Erk bands normalized to total actin, and compared with control α-CD3 stimulated cells. Data are mean ± SEM, n = 8 individual experiments. (**C**) Quantification of IL-2 production, by ELISA, compared to a standard IL-2 curve. Results are expressed as pg/mL IL-2 ± SEM; n= ten individual experiments, each in triplicate. **(D, E)** Mouse splenocytes were quantified via MTT and Trypan Blue assays. Data is expressed as a percent of control α-CD3 stimulated cells ± SEM, n = 4 individual experiments. Significance by the Student's t-test: *, $p < 0.05$; **, $p < 0.01$.
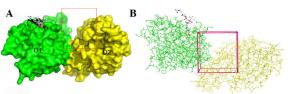
Figure 6. CD45 inhibitors arrest the DTH *in vivo*.

(**A**) Timeline for the delayed-type hypersensitivity reaction assay. Mice were primed with ovalbumin (100 µg IP, 10 µg SC) and challenged in the right footpad with the same antigen twelve days later. At the time of challenge, group A received vehicle control and group B received 3 mg/kg 211 (by intraperitoneal injection). On day 3, group C received 3 mg/kg 211. Group D was the untreated control until day 6. (**B**) Footpad swelling was measured on day 6 post-challenge and is displayed as the difference in thickness between the right (OVA challenged) and left (naïve) footpad of each mouse (mm ± SEM), pooled for each group (n=4 mice per group). Significance of ** is equivalent to $p < 0.01$ by the Student's t-test. Experimenters were blinded to the animal code.
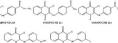
Table 1. Selectivity of inhibition of PTPases. IC_{50} for selected compounds are indicated. The highest concentration tested was 50 µM. Data are reported for experiments using pp-60 src phospho-peptide substrate (CD45) and p-NPP (LAR, PTP1B, PTP-Sigma, SHP-1 and MKPX). DIFMUP substrate (all PTP) and insulin receptor phospho-peptide (LAR) were also used as substrates, with similar results (data not shown).

| Compound | In vitro IC_{50} (µM) | | | | | |
	CD45	LAR	PTP1B	PTP-Sigma	SHP-1	MKPX
28p	4.6	12.2	2.6	8.1	0.51	12.6
37p	1.1	>50 µM	17.3	>50 µM	>50 µM	>50 µM
57p	>50 µM	>50 µM	>50 µM	>50 µM	>50 µM	>50 µM
37p analogs						
210	0.33	>50 µM	>50 µM	>50 µM	>50 µM	>50 µM
211	0.29	>50 µM	>50 µM	>50 µM	>50 µM	>50 µM
214	0.39	>50 µM	>50 µM	>50 µM	>50 µM	>50 µM
215	0.24	>50 µM	>50 µM	>50 µM	>50 µM	>50 µM
216	0.52	>50 µM	>50 µM	>50 µM	>50 µM	>50 µM

41

FIGURE 1

FIGURE 2

A. (Graph: CD45 activity (% of untreated) vs Concentration (μM), data for 28p and 37p; structure labeled COMPOUND 37p)

B. COMPOUND 210, COMPOUND 211, COMPOUND 214, COMPOUND 215, COMPOUND 216

C. (Five graphs: CD45 activity (% of untreated) vs Concentration (μM): 37p + 210; 37p + 211; 37p + 214; 37p + 215; 37p + 216)

D. (Molecular structure with residues: TYR 1001, ARG 765, ASP 760, LYS 1003, MET 999, ALA 1378, SER 1163, LEU 995, ASP 1171, V 1175, ASP 862)

E. (Bar graph: Percent CD45 Activity vs WT, K1003I, K1003A, V1175G, V1175A; legend: 1 μM 211, 10 μM 211, 10 μM RWJ)

FIGURE 3

A

B

c-terminal Src phospho-substrate Y527

C

autocatalytic Src phospho-substrate Y416

D

FIGURE 4

A.

Jurkat   J45.01
– 211   – 211

p-Lck
Y394

total
ZAP
70

B.

Jurkat   J45.01
– 211   – 211

p-Lck
Y505

total
ZAP
70

C.

Jurkat   J45.01
– 211   – 211

total
Lck

total
ZAP
70

D.

Changes induced by 211-treatment (densitometry, relative to untreated)

■ Jurkat (CD45+ve)
□ J45.01 (CD45-ve)

p-Lck Y394   p-Lck Y505   Total Lck

FIGURE 5

FIGURE 6

A.

Day -12
OVA IP, SC
immunization

Controls
Compound 211

group A (vehicle)
group B

group C

group D (untreated)

Day 0 3 6 9

OVA footpad
challenge

swelling
measurement

sacrifice

B.

Day 6 R-L footpad swelling (mm)

Group A
Vehicle control
Day 0

Group B
3 mg/kg 211
Day 0

Group C
3 mg/kg 211
Day 3

Group D
Untreated